Geometric Bargaining Approach for Optimizing Resource Allocation in Wireless Visual Sensor Networks

Katerina Pandremmenou, *Student Member, IEEE,* Lisimachos P. Kondi, *Senior Member, IEEE,* Konstantinos E. Parsopoulos, *Member, IEEE*

***Abstract*—Applications that include real-time video delivery are demanding on network performance, while the various network resources are usually constrained. This fact boosts the need for efficient resource management, aiming at the amelioration of the video quality that reaches the end-user. The present paper considers a wireless direct sequence code division multiple access visual sensor network, which employs a cross-layer design. The objective is the maximization of the nodes' utilities under the constraints of a maximum bit rate and a maximum power level for each node. In this vein, the Kalai–Smorodinsky bargaining solution is applied, which is geometrically derived from the graphical representations of the utility sets, under a centralized topology. Ultimately, we have to deal with an optimization problem that concerns the optimal determination of the source coding rates, channel coding rates, and power levels of all nodes of the network, under certain modeling conditions. The experimental results provided by the Kalai–Smorodinsky bargaining solution are compared with results using the Nash bargaining solution and two other schemes that aim at the maximization of an unweighted and a weighted version of the total network utility, respectively. A metric that captures fairness and performance issues is used in order to compare the performance of the schemes. The results are also evaluated in terms of the total consumed power relative with the total achieved utility.**

***Index Terms*—Game theory, Kalai–Smorodinsky bargaining solution, resource allocation, visual sensor network.**

I. Introduction

GAME THEORY is a branch of mathematics with extensive applications to social and formal sciences, ranging from economics to biology to computer science and other disciplines. Specifically, game theory studies the interactions of different factors in order to investigate matters such as monetary distributions in economics, the emergence of animal communication in biology, or even multiagent cooperation in artificial intelligence and resource allocation issues in various network infrastructures.

The agents that participate in a considered game sometimes coordinate their behavior to achieve a common goal, while some other times each player may follow an independent, selfish policy, aiming exclusively at its own profit. Therefore, game theory can be considered as the umbrella that encompasses two distinct branches: *cooperative* and *noncooperative* game theory. The first one studies the collective rationality of the players, while the second attempts to rationalize the selfish actions of the players.

Bargaining theory is an area of cooperative game theory that includes the notion of negotiation. Through the bargaining process, players are encouraged to choose one among many other possible outcomes, following the strategy indicated by the rational model. The outcome that determines the final share among all candidate parties constitutes a *bargaining solution*.

At this point, let us state the problem that the current paper attempts to address. We consider a wireless direct sequence code division multiple access (DS-CDMA) visual sensor network (VSN). Such networks consist of spatially distributed nodes, equipped with cameras, which monitor scenes with different motion activity. For example, some nodes may be imaging scenes with high levels of motion, while some other nodes may record low-motion scenes. VSN applications are related with video delivery, i.e., surveillance or tracking, meaning that the demands for resources are particularly increased. Therefore, an efficient allocation of the transmission parameters among all the nodes of the VSN is crucial for the overall system performance.

Assuming a centralized topology, the centralized control unit (CCU), which lies at the network layer, receives data from all source nodes and asks for adjustments to their parameters, considering their needs for both compression and error protection during transmissions. The power levels, source coding rates, and channel coding rates, which are the transmission parameters of the nodes, are determined at different network layers. Specifically, the power levels are determined at the physical layer, the channel coding rates at the data link layer and the source coding rates are selected at the application layer.

In order to overcome possible network latency problems and improve real-time system response, in this paper we assume

Manuscript received July 16, 2012; revised November 5, 2012; accepted December 19, 2012, December 27, 2012. Date of publication January 30, 2013; date of current version July 31, 2013. This work was supported in part by the Air Force Office of Scientific Research, Air Force Material Command, USAF, under Grant FA8655-12-1-0001. The U.S Government is authorized to reproduce and distribute reprints for Governmental purpose notwithstanding any copyright notation thereon. This paper was recommended by Associate Editor B. Yan.

The authors are with the Department of Computer Science, University of Ioannina, Ioannina GR-45110, Greece (e-mail: apandrem@cs.uoi.gr; lkon@cs.uoi.gr; kostasp@cs.uoi.gr).

Color versions of one or more of the figures in this paper are available online at http://ieeexplore.ieee.org.

Digital Object Identifier 10.1109/TCSVT.2013.2243646

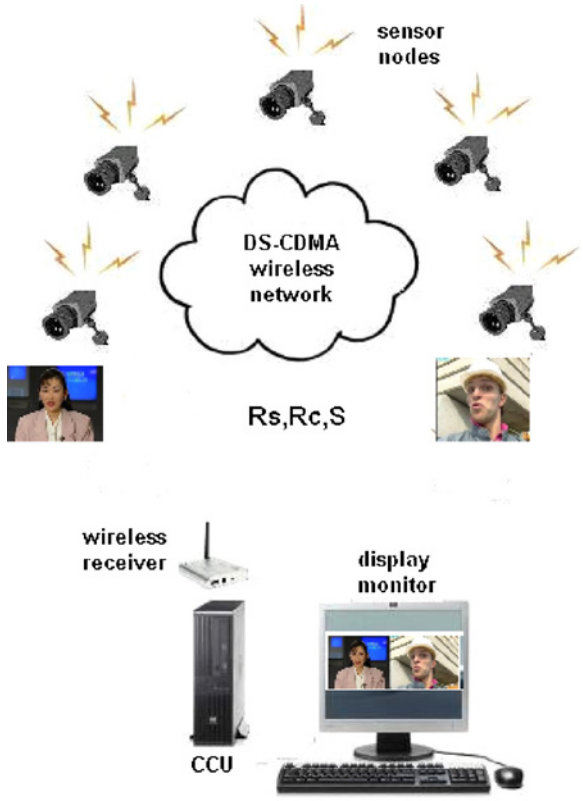

Fig. 1. DS-CDMA wireless VSN.

a flexible cross-layer design, which allows different network layers to exchange information, regardless of their position in the considered layer hierarchy. Cross-layer design has been applied in our previous works [1]–[4], significantly improving network performance. The proposed design operates across the physical, data link, network, and application layers. The CCU coordinates this layer collaboration and communicates with all nodes, receiving their data and requesting changes in their transmission parameters according to their unique, content-aware needs for resources. A typical DS-CDMA VSN is illustrated in Fig. 1.

The constraint that holds for each node of the network is that it has an available bit rate that can be shared between source and channel coding. Source coding aims at video representation with the smallest number of bits, removing redundant information from the video bitstreams. On the contrary, channel coding attempts to increase the reliability of video transmissions, and for this purpose redundant bits are added to the video bitstreams.

Additionally, each node has an available power that can be used for video sensing, processing, and transmission. Transmission powers have to be high enough to guarantee video reception with an acceptable visual quality, but on the other hand, they have to be low enough to prevent increased interference and to prolong the battery lifetime of the battery-operated nodes. Hence, the source coding rates, channel coding rates and power levels are the parameters that should be optimally determined, under certain modeling conditions, in an effort to tradeoff the video quality of the received videos and system efficacy. In this paper, the source and channel coding rates can take discrete values, while the power levels can be assigned continuous values.

Game theorists have proposed several bargaining solutions so as to resolve similar resource allocation problems. The Nash bargaining solution (NBS) was the first among many bargaining solutions. That solution, based on its set of fairness axioms provides a fair and efficient way for distributing resources.

A game-theoretic model developed in [5] is used to analyze a scenario in which the nodes of a wireless network seek to agree on a fair and efficient allocation of spectrum. For this purpose, the NBS is applied, satisfying this dual requirement. In [6], a joint subcarrier assignment and relay power allocation problem is formulated as a Nash bargaining problem with fairness consideration and practical constraints, in order to enhance system efficiency by exploiting multiuser diversity. The problem of fair and optimal bandwidth allocation among multiple collaborative video users is also solved with the help of the NBS in [7].

In our previous works [1] and [2], we have also proposed the NBS to tackle with similar problems as the one presented in this paper. Specifically, in [1], we present some early results on the use of the NBS for the cross-layer optimization of a wireless VSN. In this paper, all node parameters assume values from discrete sets and the minimum acceptable utility for the nodes is assumed to be the Nash equilibrium. The work in [2] is an extension of [1], where the source and channel coding rates assume discrete values and the power levels assume continuous values. Additionally, in the same work the minimum acceptable utility for the nodes is selected by the system designer and is not the Nash equilibrium.

In this paper, we apply the Kalai–Smorodinsky bargaining solution (KSBS) to nonconvex utility spaces, in order to find a fair utility allocation resulting from the optimal determination of the nodes' transmission parameters, considering all the assumptions and constraints of the present work. The KSBS is derived geometrically, directly from the graphical representations of the nodes' utility sets. This approach has also been applied in the past to find appropriate rules for the allocation of the available resources in various network architectures.

In [5], besides the NBS, the KSBS is also used to explore an efficient spectrum sharing for the nodes of the wireless network. The scheduling of multiple users to access channels is discussed in [6], taking into account a maximum rate constraint of each source as well as a minimum rate requirement. In that paper, both the NBS and KSBS are applied to address the problem. The problem of fair and optimal bandwidth allocation among multiple collaborative video users discussed in [7] is resolved using both NBS and KSBS. The KSBS ensures that all users incur the same utility penalty relative to the maximum achievable utility. Additionally, in [8], the KSBS is used to distribute the resources optimally and fairly among autonomous wireless stations, considering their current channel conditions, content characteristics, and cross-layer strategies.

In [9], a game theoretic approach for resource allocation using cooperative games is presented, where available network technologies cooperate to simultaneously allocate resources to

TABLE I
LIST OF ABBREVIATIONS

Abbreviation	Meaning	Abbreviation	Meaning
AVC	Advanced video voding	OFDMA	Orthogonal frequency division multiple access
AWGN	Additive white Gaussian noise	PF	Performance to fairness
BPSK	Binary phase shift keying	PSNR	Peak signal-to-noise ratio
CCU	Centralized control unit	PSO	Particle swarm optimization
DS-CDMA	Direct sequence code division multiple access	QCIF	Quarter common intermediate format
KSBS	Kalai–Smorodinsky bargaining solution	RCPC	Rate compatible punctured convolutional codes
MAI	Multiple access interference	URDCs	Universal rate distortion characteristics
MIMO	Multiple input multiple output	VSN	Visual sensor network
MTU	Maximize total utility	w.MTU	weighted maximize total utility
NBS	Nash bargaining solution		
bps	Bits per second	Hz	Hertz
dB	Decibel	W	Watts

the application requests. In that work, the KSBS determines the amount of allocation by each network technology. The application of KSBS to the problem of downlink resource allocation for multiuser multiple-input multiple-output (MIMO) orthogonal frequency division multiple access (OFDMA) systems is proposed in [10]. Additionally, [11] proposes a new system resource allocation framework for multimedia systems that perform multiple simultaneous video decoding tasks. The available system resources and the video decoding task's characteristics are jointly considered in order to determine a fair and optimal resource allocation using the KSBS.

Continuing, a fully centralized scheme based on the KSBS deals with the problem of resource allocation in wireless CDMA communication networks in [12]. A fully centralized scheme requires the base station to know all details including the users' utility, which may not always be possible. The problem of optimal allocation of bandwidth to multimedia applications within the operator network and the distribution of excess bandwidth among operators is also confronted using the KSBS in [13]. A brokerage based decentralized resource management scheme for multiuser multimedia transmission over networks is presented in [14]. In that work, the autonomous behavior of multimedia users that stream video over the networks is addressed with the Kalai–Smorodinsky approach, which explicitly considers the utility impact for different resource allocation schemes. Moreover, [15] introduces the KSBS as well as three other game-theoretic solutions which are applied as OFDMA schedulers. They are compared in two scenarios with respect to sum throughput, per user throughput, frequency band sharing and scaling with the number of users.

A significant part of the present paper is devoted to the reliable evaluation of the KSBS performance, in the quality and resource domains. Over the last few years, various fairness metrics have been proposed in the literature to weigh the video quality achieved by different resource allocation methods. In [5], the spectrum allocation achieved by the bargaining solutions is investigated using the metrics of average, minimum, and standard deviation of capacity, the KSBS score and the NBS score. In order to quantify the fairness achieved by several resource allocation schemes, an alternative fairness comparison metric is introduced in [8]. This metric is defined as the ratio of the largest quality drop among wireless stations in the network using each considered fairness scheme to the quality drop incurred by the KSBS for the wireless stations. For the KSBS, the quality drop is the same for all wireless stations.

Additionally, in [11] a quality increase factor is employed to compare the performance of the different resource allocation schemes. This factor captures the quality requirements for each task. Specifically, a factor of 0 indicates that a task achieves its minimum desired quality, while higher (positive) values of this factor indicate that the task achieves a higher quality. A quality increase factor of 100 indicates that a task achieves its maximum desired quality, and a negative quality increase factor indicates that a task achieves below its minimum required quality.

Therefore, we observe that each metric studies fairness from a different point of view, depending on the particular application as well as on the users' desires. In the present paper, we apply a metric that captures both performance and fairness aspects [16], [17] in order to estimate the behavior of the proposed method. On the grounds that a desirable resource allocation policy is one that achieves high total utility, behaves equally fairly to all nodes, and requires low levels of power, we study the total consumed power relatively with the total utility gain in order to evaluate the results in the resource domain. The performance of the KSBS criterion was examined in comparison with the NBS criterion. Both of these solutions, satisfying a set of axioms, offer a compromise between efficiency and fairness. In our previous work [18], promising preliminary results regarding the performance of the KSBS offered strong motivation for the further investigation of the aforementioned resource allocation problem, while these results were juxtaposed with the results obtained from the implementation of the NBS [2].

Moreover, we also compare the KSBS results with results using two alternative schemes that maximize the total system utility achieved by all nodes of the network. The first scheme calculates an *unweighted* version of the total system utility and is called the maximize total utility (MTU) criterion [5], [8], [19], [20]. Similarly to our work, in [5] the bargaining solutions are compared with the allocation that maximizes the sum of channel capacities, besides the other proposed metrics. In [8], the maximum total system quality is one of

the strategies that is compared with the KSBS for the problem of optimal resource distribution among autonomous wireless stations. The maximum total system quality, as declared by its name, leads to the maximum sum of the wireless stations qualities, while the quality difference between the wireless stations is significant. The work in [19] analyzes scenarios in which self-interested agents negotiate with each other in order to agree on deals to exchange resources. In the same paper, the authors identify the welfare enjoyed by a society of agents with the sum of the values ascribed by the individual agents in that society to the resources they hold in a particular situation. The behavior modeling and analysis of the dynamics in a colluders' social network in order to achieve different fairness of collusion is studied in [20]. In that work, human behavior is analyzed by four bargaining criteria. According to the max-sum solution, all the members in the colluders' social network have the same goal so that they are willing to maximize the total utility over the whole social network.

Additionally, the second scheme we compare with the KSBS results calculates a weighted version of the overall system utility, and is called the weighted maximize total utility (w.MTU) [21]–[23]. In [21], an optimal feedback allocation policy for cellular uplink systems is proposed where the base station has a limited feedback budget. The optimal allocation policy of this paper involves solving a weighted sum-rate maximization problem at every scheduling instant. The work presented in [22] studies the multiuser resource allocation problem in OFDMA networks, extending the traditional network utility maximization problem into a more general framework of weighted network utility maximization. Furthermore, in [23] a joint subcarrier and power allocation algorithm is proposed for maximizing the weighted sum rate in multiuser OFDMA downlink systems.

The mixed-integer optimization problems resulting from the discrete values of the source and channel coding rates, and the continuous values of the power levels were tackled for the NBS, MTU, and w.MTU with the help of the particle swarm optimization (PSO) algorithm [2], [3], [24], [25]. PSO belongs to the category of population-based algorithms and is a stochastic algorithm for numerical optimization tasks.

Summarizing, the core of the present paper includes the determination of source coding rates, channel coding rates, and transmission powers of the nodes, under the constraint of a maximum bit rate for each node. The KSBS is the tool applied in this paper to optimally determine the aforementioned parameters. The optimality is subject to the modeling assumptions made, the constraint on the maximum bit rate, and the definition of the sets of admissible source coding rates, channel coding rates, and power levels. This criterion eventually offers a solution that satisfies all nodes, providing acceptable levels of viewing quality for the videos captured by all of them. Since there are many abbreviations and notations in this paper, we summarize abbreviations in Table I and notations in Table II accompanied by their meaning, for reader's convenience.

The rest of the paper is organized as follows. Section II describes the channel access method used by the nodes as well as the main characteristics of source and channel coding. In Section III, the model used to calculate the expected video distortion is analyzed. Section IV provides the theoretical background of game theory, while in Section V, the proposed bargaining solution is presented. Section VI includes the evaluation metrics for the quality and resource domains, and in Section VII, the system parameters are defined and the experimental results are presented, accompanied by their interpretation. Finally, Section VIII summarizes the key concepts and conclusions of our investigation.

II. Visual Sensor Network

In this section, we analyze the DS-CDMA channel access method and present the main features of source and channel coding.

A. Direct Sequence Code Division Multiple Access

The VSN considered in this paper consists of a number of spatially distributed nodes. Each of the nodes has a camera in order to monitor scenes with varying amounts of motion. The channel access method employed by the nodes of this paper is DS-CDMA. Each node is assigned a unique spreading code, often orthogonal or pseudorandom to the codes assigned to the other nodes, such that the interference between the signals is minimized. In order to transmit a single bit, a node actually transmits L chips, where L is the spreading code length, measured in chips. Usually, the chip rate, R_{chip}, which is the number of transmitted chips per second, measured in chips per second, is identical for all nodes. In this paper, we assume that the spreading code length is also identical for the nodes. Thus, since the bit rate, R_k, for node k, is equal to the ratio $R_k = R_{\text{chip}}/L$, a constraint on the chip rate corresponds to a constraint on the bit rate.

Furthermore, it also holds that $R_k = R_{\text{s},k}/R_{\text{c},k}$. This means that the total bit rate also equals the ratio of the source coding rate, $R_{\text{s},k}$, to the channel coding rate $R_{\text{c},k}$, for each node k. The bit rate R_k and the source coding rate $R_{\text{s},k}$ are measured in bits per second (bps). The channel coding rate $R_{\text{c},k}$ is a dimensionless number, smaller than unity [26] and corresponds to the number of input bits to the channel coder over the number of output bits. Thus, for fixed R_k, the higher the source coding rate for a video sequence, the lower the video sequence protection from channel errors, and vice versa.

The use of DS-CDMA allows all nodes to transmit over the same channel, without a hard limitation on the number of nodes that can access the same channel at the same time. Generally, the multiple, simultaneous transmissions over the same channel cause interference among the nodes, which can be ascribed to nonorthogonal spreading codes, asynchronous transmissions, and multipath fading. Hence, it is necessary to control the transmission power in order to balance the tradeoff between limited interference among nodes' transmissions and high video viewing quality.

The power level S_k, for node k, determines the power that is received by the CCU, after a node's transmission. It is given by $S_k = E_k R_k$, and is measured in Watts (W). The quantity E_k is the energy per bit. In order to compute the transmission power, we have to adopt a propagation model. If we assume

the two-ray ground reflection model, the transmission power, $S_{k_{\text{trans}}}$, for node k, is given by [27]

$$S_{k_{\text{trans}}} = \frac{S_k\, d_{\text{tr}}^4}{G_{\text{t}}\, G_{\text{r}}\, h_{\text{t}}^2\, h_{\text{r}}^2} \tag{1}$$

where d_{tr} is the distance between the transmitter (node) and the receiver (CCU), G_{t} is the transmitter antenna gain, G_{r} is the receiver antenna gain, h_{t} is the height of the transmitter antenna, and h_{r} is the height of the receiver antenna.

In our investigation, we followed the assumption that the interference can be approximated by additive white Gaussian noise (AWGN) [28]. Assuming that thermal and background noise are significant compared to the interference, the energy per bit to multiple access interference (MAI) and noise ratio, $E_k/(I_0 + N_0)$, for node k, is given by

$$\frac{E_k}{I_0 + N_0} = \frac{S_k/R_k}{\sum_{j \neq k}^{K} S_j/W_t + N_0}, \qquad k = 1, 2, \ldots, K \tag{2}$$

where $I_0/2$ is the two-sided noise power spectral density due to MAI and $N_0/2$ is the two-sided noise power spectral density of the thermal and background noise, measured in Watts/Hertz (W/Hz). The amount W_t is the bandwidth, measured in Hertz (Hz).

B. Source and Channel Coding

Channel capacity is usually a limited network resource, meaning that data representation with the smallest possible number of bits is an imperative need. Due to this, source coding is applied before data is conveyed through the network. Certainly, the compression requirements vary per video sequence, while the end-user can also determine which video sequences are source encoded at a higher rate, for each considered application.

For example, if the end-user feels that some sensor nodes monitor more interesting scenes compared to some others, he/she will require these nodes to enhance the quality of the video they record. This means that more bits will be spent for compression in order to avoid significant degradation of the video quality. Hence, fewer bits will be available for channel coding, implying lower error protection. The video sequences captured by the nodes of our study were compressed using the H.264/advanced video coding (H.264/AVC) standard, in combination with the 4:2:0 High Profile for chroma subsampling. The aforementioned coding standard is an extremely efficient tool for coding, considering the available coding tools for the encoder provided by the 4:2:0 High Profile [29].

Channel coding aims at increasing channel reliability. Specifically, channel codes add redundant bits to video sequences in order to achieve a more error-resistant system. In cases where a video sequence uses fewer bits for error protection, it is necessary to increase the transmission power in order to keep the bit error rate at acceptable levels. In this paper, we employed rate-compatible punctured convolutional (RCPC) codes [30], which are families of codes with different rates. However, other channel coding schemes can also be used. The RCPC codes allow us to utilize Viterbi's upper bounds on the bit error probability, P_{b}, which is described by the inequality [30]

$$P_{\text{b}} \leqslant \frac{1}{P} \sum_{d=d_{\text{free}}}^{\infty} c_d\, P_d. \tag{3}$$

The parameter P is the period of the code, d_{free} is the free distance of the code, c_d is the information error weight, and P_d is the probability that the wrong path at distance d is selected.

In an AWGN communication channel where the modulation scheme used is binary phase shift keying (BPSK), the probability P_d equals [30]

$$P_d = \frac{1}{2} \operatorname{erfc}\left(\sqrt{\frac{d R_{\text{c}} E_k}{I_0 + N_0}}\right) \tag{4}$$

where

$$\operatorname{erfc}(x) = \frac{2}{\sqrt{\pi}} \int_x^{\infty} \exp\left(-t^2\right) dt$$

is the complementary error function, R_{c} is the channel coding rate, and $E_k/(I_0 + N_0)$ the energy per bit normalized to the MAI and noise ratio, described in (2). The index k declares the corresponding node of the network.

III. Expected Video Distortion

After data transmission from the source nodes to the CCU, the video quality is inevitably degraded. This fact is ascribed to lossy compression and the errors introduced by the channel. Therefore, the bit error rate, or else, the bit error probability, P_{b}, affects video distortion, and thus, it has an immediate impact on the video viewing quality.

A useful tool that relates P_{b} with the expected video distortion, $E[D_{\text{s+c},k}]$, after channel decoding, is the universal rate distortion characteristics (URDCs) [31], for which we assume the following model:

$$E[D_{\text{s+c},k}] = \alpha \left[\log_{10}\left(\frac{1}{P_{\text{b}}}\right)\right]^{-\beta}. \tag{5}$$

The α and β are two positive parameters, which are highly dependent on the motion level of each video sequence and the source coding rate. Particularly, the higher the source coding rate or the higher the motion level of a video sequence, the higher the α value. The values of α and β are determined in a preprocessing phase by using mean squared error optimization for some $(E[D_{\text{s+c},k}], P_{\text{b}})$ pairs [4].

In Section II-A, we discussed about the constraint that is placed on the total available bit rate for each node. We mentioned that for fixed bit rate, the higher the source coding rate for a video sequence, the lower the video sequence protection during transmission through the channel, and vice versa. Hence, source coding rates and channel coding rates are two interdependent variables that can be considered as a pair in the present paper. Let the index cb denote the admissible source coding rate-channel coding rate combinations. Each source–channel coding rate combination, $cb = 1, 2, \ldots, CB$, assumes values from a set

$$\mathbf{R}_{\text{s+c}} = \big\{(R_{\text{s},k,1}, R_{\text{c},k,1}), \ldots, (R_{\text{s},k,cb}, R_{\text{c},k,cb}), \ldots, (R_{\text{s},k,CB}, R_{\text{c},k,CB})\big\}$$

$$E[D_{\mathrm{s+c,k}}](R_{\mathrm{s},k}, R_{\mathrm{c},k}, S) = \alpha(cb)\left[\log_{10}\frac{1}{\frac{1}{P}\sum_{d=d_{\mathrm{free}}(cb)}^{\infty}\left(c_d(cb)\frac{1}{2}\mathrm{erfc}\left(\sqrt{dR_{\mathrm{c},k}\left(\frac{\frac{S_k}{R_k}}{\sum_{j\neq k}^{K}\frac{S_j}{W_t}+N_0}\right)}\right)\right)}\right]^{-\beta(cb)} \tag{6}$$

where the cardinality of $\mathbf{R}_{\mathrm{s+c}}$ is equal to CB. For the channel coding rates, we assumed discrete values [30] from a set $\mathbf{R_c}$, and thus the source coding rates can also take discrete values from a set $\mathbf{R_s}$. This fact implies that the source–channel coding rate combinations also assume discrete values. Furthermore, the sets $\mathbf{R_s}$, $\mathbf{R_c}$ and $\mathbf{R}_{\mathrm{s+c}}$ have the same cardinality. An increase in the cardinality of the sets, results in a significant increase of the search space, with a consequent impact on the corresponding problem's difficulty. For the power levels, we assumed that they can take continuous values from a set of predetermined range, i.e., $S_k \in \mathbf{P} = [p_{\min}, p_{\max}] \subset \mathbb{R}$, for node k.

As we mentioned before, the parameters α and β of (5) depend on the source coding rate. Additionally, the parameters d_{free} and c_d of (3) depend on the channel coding rate. Thus, all the aforementioned parameters dependent on cb. Substituting (4) into (3) (with equality), and (3) into the URDCs model, the expected video distortion, $E[D_{\mathrm{s+c},k}]$, is finally given by (6) for node k. Obviously, the expected video distortion is a function of the source coding rate, $R_{\mathrm{s},k}$, channel coding rate, $R_{\mathrm{c},k}$, as well as of the power levels, $S = (S_1, S_2, \ldots, S_K)^{\top}$, of all nodes of the network. Eventually, it suffices to determine the source–channel coding rate combinations, and the power levels of the nodes.

IV. Review of Game Theory

Game theory studies people's interactions in a considered game, which can be either conflicting or coordinated. Cooperative game theory investigates coalitional games with respect to the advantage that each player has in the considered game, while it also studies the way that the overall payoff is divided among the players of the game. On the contrary, noncooperative game theory is mainly concerned with the selfish behavior on behalf of the players, aiming at the maximization of their own profit.

In the current paper, the considered game is the resource allocation game, i.e., the allocation of the source coding rates, channel coding rates, and power levels to all nodes of the network, which play the role of the players. Increasing the transmission power of one node will improve its received video quality. However, the increased interference will reduce the video quality of the other nodes.

In order to tackle the aforementioned problem, we apply axiomatic bargaining game theory [32], with the goal of maximizing the quality of the transmitted video that reaches the end-user. Axiomatic bargaining defines a set of axioms that the optimal solution should satisfy. In this way, all but one candidate solutions are rejected, since they fail to satisfy all axioms. Thus, a unique optimal solution is finally selected.

The utility function, U_k, constitutes a measure of relative satisfaction for each node k. In this paper, this quantity is defined similarly to the peak signal-to-noise ratio (PSNR), as follows [2], [18]:

$$U_k = 10\log_{10}\frac{255^2}{E[D_{\mathrm{s+c},k}]}, \quad k = 1, 2, \ldots, K \tag{7}$$

and it is thus measured in decibel (dB). The $E[D_{\mathrm{s+c},k}]$ corresponds to the expected video distortion given by (6). Since U_k defines the preference for node k, it follows that the higher the U_k value, the higher the profit for the node.

From (7), we observe that the utility function is related with the expected video distortion, which is a function of the source coding rates, channel coding rates, and power levels of the nodes. Each combination of these parameters corresponds to a value for the utility of node k. The vector $U = (U_1, U_2, \ldots, U_K)^{\top}$ consists of the utilities of all K nodes. The feasible set $\mathbf{U}$ encompasses all possible vectors U.

In our investigation, for the feasible sets we allowed the use of pure strategies only, which define deterministic actions for the nodes [33]. These sets have to satisfy the following conditions [5].

1) $\mathbf{U} \subset \mathbb{R}^K$ is Z-comprehensive, closed and bounded-above.
2) Free disposal is allowed.

According to the first condition, the set $\mathbf{U}$ is said to be Z-comprehensive if $X, Y \in \mathbb{R}^K$, such that $Z \leq X \leq Y$, then $Y \in \mathbf{U}$ implies $X \in \mathbf{U}$. When free disposal is allowed for a feasible set, this means that each node is permitted to dispose of utility at will. This fact implies that the feasible set $\mathbf{U}$ is also Z-comprehensive [5], [33]. In the case of video, this means that a node has the option to purposely add noise to its video to degrade video quality. This is obviously not a wise choice on behalf of the nodes and will never be chosen. Nevertheless, we should not exclude any utility allocations from the utility set, unless these utility allocations are impossible to be achieved.

TABLE II
LIST OF NOTATIONS

Notation	Meaning	Notation	Meaning
α	Model parameter	$\max U_k$	Maximum possible utility for node k
$\alpha_1, \alpha_2, \alpha_3$	Coefficients of the polynomial	N_{cl}	Cardinality of class cl
a_{cl}	Bargaining power/weight for class cl	N_0	AWGN
β	Model parameter	P	Period of the code
C	Number of motion classes	$\mathbf{P}$	Set of power levels
cb	Source–channel coding rate combination	P_{b}	Bit error probability
c_d	Information error weight	P_d	Probability of selecting the wrong path at distance d
$Cons$	Each considered scheme	$PSNR_k$	PSNR for node k
d_{free}	Free distance	$\mathbf{R_c}$	Set of channel coding rates
dp	Disagreement point	R_{chip}	Chip rate
d_{tr}	Distance between transmitter and receiver	$\mathbf{R_s}$	Set of source coding rates
erfc	Complementary error function	$\mathbf{R}_{\mathrm{s+c}}$	Set of source and channel coding rate combinations
$E[D_{\mathrm{s+c},k}]$	Expected video distortion for node k	$R_{\mathrm{c},k}$	Channel coding rate for node k
E_k	Energy per bit for node k	R_k	Bit rate for node k
$E_k/(I_0 + N_0)$	Energy per bit to MAI and noise ratio for node k	$R_{\mathrm{s},k}$	Source coding rate for node k
$F(\mathbf{U}, dp)$	Kalai–Smorodinsky bargaining solution	S_k	Power level for node k
G_{r}	Receiver antenna gain	$S_{k_{\mathrm{trans}}}$	Transmission power for node k
G_{t}	Transmitter antenna gain	U	Vector of utilities
h_{r}	Receiver antenna height	$\mathbf{U}$	Feasible set
h_{t}	Transmitter antenna height	U_k	Utility for node k
K	Number of nodes	$U_{MAX}(\mathbf{U}, dp)$	Utopian point
L	Spreading code length	W_t	Bandwidth

Each utility allocation comes from a different combination of the nodes' transmission parameters, resulting in a different utility assignment for each node.

A resource allocation outcome is strongly Pareto-optimal if there cannot be another feasible outcome which is strictly preferred by at least one node, and weakly preferred by the other nodes. In other words, this means that all nodes maintain the payoff they hold and at least one node increases its utility. Instead, a weakly Pareto-optimal allocation of resources is strictly preferred by all the nodes of the network, meaning that all of them increase their utilities [33]. All the points that are characterized as Pareto-optimal, strongly and/or weakly, are points of the feasible set and consist the bargaining set, which is thus a subset of the feasible set.

In bargaining theory, disagreement point is called the policy that is implemented if no agreement is reached. Concerning the resource allocation problem, if the nodes of the network decide to not cooperate with each other, the disagreement point guarantees the minimum utility assigned to each of them.

More specifically, it is the vector of minimum utilities defined as

$$dp = (dp_1, dp_2, \ldots, dp_K)^{\top} \tag{8}$$

where dp_k is the minimum acceptable utility for node k, and $dp \in \mathbf{U}$. Evidently, the value of the disagreement point has a profound impact on the outcome of negotiations, even if it never comes to pass.

The vector that consists of the maximum achievable utilities that each node can get by participating in the resource allocation game is called utopian point, and is defined as

$$U_{MAX}(\mathbf{U}, dp) = (\max U_1, \max U_2, \ldots, \max U_K)^{\top} \geq dp. \tag{9}$$

The maximum possible utility, $\max U_k$, for node k, has to be greater or at least equal to the utility that node k can get at its disagreement point, dp_k. Since the available resources are usually limited, it is impossible for all nodes to benefit at the same time. Therefore, the utopian point does not belong to the feasible set.

V. PROPOSED METHOD

This section is devoted to the Kalai–Smorodinsky bargaining solution. We also discuss the geometric approach that was followed in order to reach the desirable solutions.

A. Kalai–Smorodinsky bargaining solution

The Kalai–Smorodinsky bargaining solution $F(\mathbf{U}, dp)$, for the feasible set $\mathbf{U}$, and the disagreement point dp, is the solution that satisfies the following axioms [18], [33], [34]:

1) $F(\mathbf{U}, dp) \geq dp$.
2) $Y \gg F(\mathbf{U}, dp) \Rightarrow Y \notin \mathbf{U}$.
3) Given any strictly increasing affine transformation $\tau()$, it holds that $F(\tau(\mathbf{U}), \tau(dp)) = \tau(F(\mathbf{U}, dp))$.
4) Suppose that $dp \in \mathbf{U}' \subseteq \mathbf{U}$ and U_{MAX} is identical for both $(\mathbf{U}, dp)$ and $(\mathbf{U}', dp)$. Then, if $F(\mathbf{U}', dp)$ is a Pareto-optimal point of $\mathbf{U}$, it holds that $F(\mathbf{U}, dp) = F(\mathbf{U}', dp)$.

The first two axioms state that the bargaining solution lies in the bargaining set. Particularly, the second one specifies that the solution $F(\mathbf{U}, dp)$ is weakly Pareto-optimal, i.e., if there is a point Y that is strictly preferred by all nodes, then Y does not belong to the feasible set. The third condition stipulates that if the utility function or the disagreement point are scaled by an affine transformation, the bargaining solution remains unaffected. The axiom of strong individual

monotonicity, described by the fourth axiom, presents the circumstances under which two sets have the same solution.

According to [35], the KSBS is found by taking the maximal element of the feasible set (lying on the bargaining set), on the line connecting the disagreement point and the utopian point (Fig. 2). It should be stressed that the KSBS can be applied either to convex or to nonconvex feasible sets, satisfying the aforementioned conditions. The only difference lies in the weak/strong Pareto-optimality axiom, which holds for nonconvex/convex feasible sets, respectively. As mentioned earlier, weak Pareto-optimality declares that all nodes prefer the payoff they get with Y more than the payoff they get with $F(\mathbf{U}, dp)$. Strong Pareto-optimality means that all nodes like Y at least as much as $F(\mathbf{U}, dp)$ and that at least one node likes Y strictly more than $F(\mathbf{U}, dp)$. In this paper, experimentation proved that the examined feasible sets were all slightly nonconvex sets, and due to this, the KSBS has to satisfy the condition of weak Pareto-optimality [5], [18], [34].

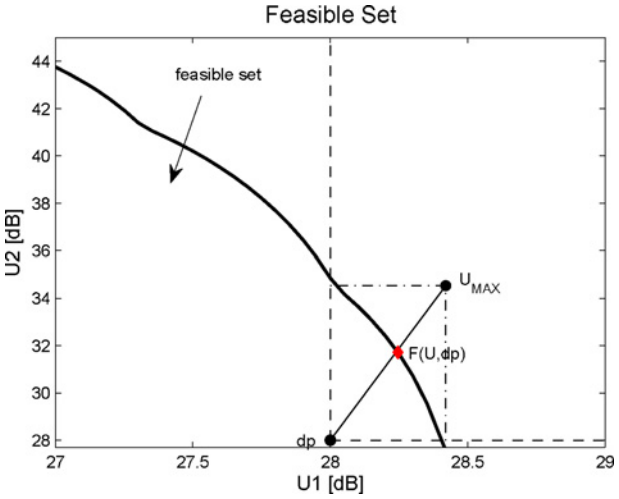

Fig. 2. Feasible set and the KSBS.

B. Geometric Approach

Let us now describe the procedure that we followed in order to solve the problem under investigation. We seek the rule that allocates fairly and efficiently the discrete source and channel coding rates, and the continuous power levels among all the nodes of the network. This rule is defined by the KSBS, which is calculated at the CCU. For simplicity reasons, we grouped the nodes into $C = 2$ motion classes, based on the amount of motion in the scenes they detect. However, other values of C can also be used. Hence, two motion classes were formed. A high-motion class consisting of the nodes that detect high levels of motion and a low-motion class consisting of the nodes that detect low levels of motion.

Since the KSBS is found by taking the element of the bargaining set that also lies on the line that connects the disagreement point and the utopian point, we approach the problem of the current paper under a geometric perspective. The bargaining solutions are derived geometrically, directly from the graphical representation of each considered feasible set.

Fig. 2 gives a useful intuition about the feasible set and the KSBS. Specifically, it depicts the feasible set $\mathbf{U}$, when there are two classes of nodes in the network. U_1 declares the utility for the first class of nodes and U_2 for the second class of nodes. In our work, these quantities represent the corresponding PSNR values for each class of nodes. The utopian point U_{MAX} lies outside the feasible set, as it was anticipated. In the same figure, the diamond represents the KSBS, $F(\mathbf{U}, dp)$, for the feasible set $\mathbf{U}$ and the disagreement point dp.

A feasible point results from a combination of the nodes' transmission parameters. Thus, considering all possible combinations of the transmission parameters, we have the feasible set. In the following, in order to determine the bargaining set, namely the Pareto-optimal points of the feasible set, we partition the x-axis of the feasible set in small, equal segments. For each segment of the x-axis, we keep the point with the highest value in the y-axis. The set that is formed including the points with the highest values in the y-axis, for each segment of the x-axis, forms the bargaining set. In order to find the equation that describes the bargaining set, a polynomial of second degree is used, since it is a good approximation for this set. Specifically, we have the equation

$$U_2 = \alpha_1 U_1^2 + \alpha_2 U_1 + \alpha_3 \tag{10}$$

where the coefficients $\alpha_1, \alpha_2, \alpha_3$ are estimated in a least square sense for a few (U_1, U_2) pairs.

In the following, we set the disagreement point at a specific value and we compute the vector of the utopian point, $U_{\mathrm{MAX}}(\mathbf{U}, dp)$, which corresponds to the maximum achievable utilities for each class of nodes. We connect the disagreement point with the utopian point with a straight line and find the equation of this line. Specifically, we have the equation

$$U_2 = \frac{\max U_2 - dp_2}{\max U_1 - dp_1}(U_1 - dp_1) + dp_2. \tag{11}$$

Therefore, having a set of equations, (10) and (11), we solve the system. The point that results from solving the system is the intersection point of the curve and the straight line and corresponds to the Kalai–Smorodinsky bargaining solution that we seek to find. This point belongs to the bargaining set and is unique, as we can see for example in Fig. 2. Therefore, it is a Pareto-optimal point. Concisely, the steps for the calculation of the KSBS are described in Algorithm 1.

As previously mentioned, each feasible point comes from a combination of the nodes' transmission parameters. Specifically, in our problem, it corresponds to a power level value and a combination of source and channel coding rate values, assuming a maximum power constraint and a fixed bit rate constraint. Allowing continuous values for the power levels, we have an infinite number of points in the feasible set. Thus, in order to graphically determine the KSBS, discretization of the power levels is necessary. Therefore, we constrain the power levels to take values within a set of predetermined range, with a step size equal to 10^{-1}.

Clearly, the smaller the step size, the higher the computational complexity of the problem and vice versa. Due to this fact, in this paper we chose the value of 10^{-1} for the step size of the power levels. This assumption has minor and trivial

Algorithm 1 KSBS Calculation

1. Determine all feasible points (U_1, U_2).
2. Determine the feasible points (U_1, U_2) that form the bargaining set.
3. Determine the coefficients $\alpha_1, \alpha_2, \alpha_3$ of $U_2 = \alpha_1 U_1^2 + \alpha_2 U_1 + \alpha_3$, in a least square sense for a few (U_1, U_2) feasible points.
4. Determine $dp = (dp_1, dp_2)^\top$.
5. Determine $U_{MAX}(\mathbf{U}, dp) = (\max U_1, \max U_2)^\top$.
6. Connect dp and $U_{MAX}(\mathbf{U}, dp)$ with a straight line.
7. Find $U_2 = \frac{\max U_2 - dp_2}{\max U_1 - dp_1}(U_1 - dp_1) + dp_2$.
8. Solve the system of $U_2 = \alpha_1 U_1^2 + \alpha_2 U_1 + \alpha_3$ and $U_2 = \frac{\max U_2 - dp_2}{\max U_1 - dp_1}(U_1 - dp_1) + dp_2$.
9. $F(\mathbf{U}, dp)$ is the intersection point of the system.

effects on the achieved performance for the nodes, incurring solutions for the PSNR values with differences to the third or fourth decimal digit compared to the PSNR values obtained after assuming a smaller step size i.e., 10^{-3} or 10^{-4}. In our opinion, these utility differences are negligible compared to the great gain of the problem's complexity reduction and clearly, this quality difference can not be perceived by the human eye.

VI. Evaluation Metrics

This section presents the metric used for the quality evaluation of the results as well as an interpretation of the results from the perspective of power consumption relative with the total achieved utility.

A. System Evaluation in the Quality Domain

Assuming that the criterion that maximizes the unweighted version of the total system utility, namely the MTU, is used as the reference criterion, we define the performance to fairness (PF) metric [16], [17] as

$$PF(MTU, Cons) = \frac{\sum_{cl=1}^{C}(U_{cl}^{MTU} - U_{cl}^{Cons})}{\sum_{cl=1}^{C}\max(0, U_{cl}^{Cons} - U_{cl}^{MTU})} \quad (12)$$

where *Cons* refers to each considered scheme and *cl* declares each considered class of nodes of the C motion classes. The numerator of the above equation quantifies the total performance gain of using the MTU over *Cons* and the denominator quantifies the unfairness of using the MTU over *Cons*.

B. System Evaluation in the Resource Domain

In order to make a more reliable estimation about the fairness and performance of the KSBS, we also evaluate each tested scheme in the resource domain (power consumption). Specifically, a desirable scheme could combine high total utility, fairness, and low levels of power consumption for all nodes. Inspired by this fact, for each of the KSBS, NBS, MTU and w.MTU, we estimate the total power consumption, cumulatively for all nodes, grouped into C motion classes, that is

$$\sum_{cl=1}^{C} S_{cl} \quad (13)$$

where S_{cl} represents the power level of class *cl*. Therefore, we study the total power consumption in combination with the total utility, for each examined scheme.

VII. System Setup and Experimental Results

This section discusses the parameter settings and also presents the experimental results accompanied by their interpretation.

A. Configuration of the System Parameters

In this paper, we assume that the network consists of $K = 100$ nodes grouped into $C = 2$ motion classes based on the amount of motion in the detected scenes, while other values of C can also be used. Therefore, two motion classes are formed. A high-motion class consisting of the nodes that monitor scenes with high levels of motion, which is represented by the *Foreman* video sequence, and a low-motion class consisting of the nodes that image scenes with low levels of motion, which is represented by the *Akiyo* video sequence.

In cases where the nodes that record low motion suddenly record an event with high motion, a new node clustering is required to achieve a reliable and optimal resource allocation. The same also holds for the cases where the nodes that image high motion instantaneously image a scene with virtually no detected motion. The resolution for both video sequences is the quarter common intermediate format (QCIF), and the URDCs are obtained at a frame rate of 15 frames per second.

The RCPC codes used for channel coding have a mother code of rate 1/4 [30]. Given that the bit rate constraint is $R_k = 96$ kbps and considering a node clustering into two motion classes, it follows that the source–channel coding rate combinations per motion class can take the following values: $\{(R_{s,1}, R_{c,1}), (R_{s,2}, R_{c,2})\} \in \{(32, 1/3), (48, 1/2), (64, 2/3)\}$. The pair $(R_{s,1}, R_{c,1})$ is the combination of the source and channel coding rates for the high-motion class of nodes and the $(R_{s,2}, R_{c,2})$ corresponds to the same parameters for the low-motion class of nodes. The power levels take continuous values from the set $\mathbf{P} = [5.0, 15.0]$ W. For the bandwidth, we examine the values of $W_t = 20$ MHz and $W_t = 15$ MHz.

All the presented results have been obtained using simulations. The results of the KSBS are compared with the corresponding results of the NBS, MTU, and w.MTU. The NBS is able to provide a Pareto-optimal solution, adhering to a set of four axioms [2], [33]. The three of the four axioms for this solution coincide with the first three axioms described in Section V-A for the KSBS. The difference lies on the fourth axiom, where the axiom of strong individual monotonicity for the KSBS is replaced by the axiom of independence of irrelevant alternatives for the NBS. According to the axiom of independence of irrelevant alternatives, if $dp \in \mathbf{Y} \subseteq \mathbf{U}$, then $F(\mathbf{U}, dp) \in \mathbf{Y} \Rightarrow F(\mathbf{Y}, dp) = F(\mathbf{U}, dp)$. This means that if

the bargaining solution, $F(\mathbf{U}, dp)$, for the feasible set $\mathbf{U}$ also belongs to a subset $\mathbf{Y}$ of the feasible set, then $F(\mathbf{Y}, dp)$ shall be the same as $F(\mathbf{U}, dp)$, since none of the extra elements of $\mathbf{U}$ were chosen as a solution when they were available. Thus, their unavailability in $\mathbf{Y}$ should be irrelevant.

The NBS for the two motion classes can be found by maximizing the Nash product

$$F(\mathbf{U}, dp) = \arg \max_{U \geqslant dp} [(U_1(R_{s,1}, R_{c,1}, S) - dp_1)^{a_1} (U_2(R_{s,2}, R_{c,2}, S) - dp_2)^{a_2}] \quad (14)$$

such that $a_1 + a_2 = 1$. The subscript 1 denotes the high-motion class of nodes, while 2 the low-motion class of nodes. The parameters a_1 and a_2 represent the bargaining powers assigned to the high- and low-motion class of nodes, respectively. The bargaining powers declare the relative advantage that each class of nodes has in the negotiation. We assume that the bargaining powers are proportional to the number of nodes in each class [2]. Thus, $a_1 = N_1/K$ and $a_2 = N_2/K$, where N_1 represents the number of nodes in the high-motion class and N_2 the number of nodes in the low-motion class.

The MTU and w.MTU both aim at the maximization of the total system utility. Specifically, the MTU maximizes

$$\max [U_1(R_{s,1}, R_{c,1}, S) + U_2(R_{s,2}, R_{c,2}, S)]. \quad (15)$$

The w.MTU assumes weights for each class of nodes that are proportional to the cardinality N_{cl}, of each class cl. Therefore, the resulting equation under maximization is:

$$\max [a_1 U_1(R_{s,1}, R_{c,1}, S) + a_2 U_2(R_{s,2}, R_{c,2}, S)] \quad (16)$$

where the weight a_1 equals $a_1 = N_1/K$ and the weight a_2 equals $a_2 = N_2/K$.

The optimization tool that the NBS, MTU, and w.MTU use to solve the mixed-integer optimization problem that results from the discrete source and channel coding rate combinations and the continuous power levels is the PSO algorithm [24], [25], with the same parameter settings as in [2] and [3]. In all conducted experiments, we assume that the thermal and background noise can be modeled as AWGN with $N_0 = 10^{-7}$ W/Hz. For values of N_0 smaller than 10^{-7}, a marginal PSNR increase is anticipated, which is trivial and unperceivable by the human eye. Additionally, $PSNR_{cl}$, which corresponds to the utility U_{cl} for class of nodes cl, is used to assess the perceived video quality of the *Foreman* and *Akiyo* video sequences.

B. Presentation and Discussion of Results

A large part of our experimental results are organized into tables. Each row of the tables refers to a specific node distribution, which is denoted as $N_1 - N_2$, where $N_1, N_2 \in \{10, 30, 50, 70, 90\}$ and $N_1 + N_2 = K = 100$. This means that the high-motion class consists of N_1 nodes and the low-motion class of N_2 nodes, respectively.

Table III explores the effect of assigning different dp values to the results of the KSBS. The terms $PSNR_1$ and $PSNR_2$ refer to the PSNR achieved by the high- and low-motion class, respectively. It can be seen that higher dp values favor the high-motion class and lower dp values favor the low-motion class. Videos with more intense motion activity are generally considered as more important compared to more stationary videos, since such videos image scenes of interest. Therefore, aiming at better video quality for the high-motion scenes, we choose to initialize dp with the highest values among the tested ones for each bit rate and bandwidth combination. Specifically, for $R_k = 96$ kbps and $W_t = 20$ MHz, the selected dp value is $dp = (28, 28)^\top$ dB, while for $R_k = 96$ kbps and $W_t = 15$ MHz, the selected dp value is $dp = (26, 26)^\top$ dB. It is worth mentioning that it is not necessary for the dp to have the same value for both motion classes. However, we make this assumption in an effort to be equally fair to all of them.

Also, from Table III, we infer that the PSNR values for both motion classes are reduced when the bandwidth is reduced, while the bit rate, N_0 and the disagreement point remain the same. This is attributed to the fact that when the bandwidth W_t is reduced, the term I_0, which is equal to $I_0 = \sum_{j \neq k}^{K} S_j / W_t$, increases. Thus, the energy per bit to MAI and noise ratio of (2) becomes lower, which leads to reduced PSNR values.

Furthermore, Table IV includes the results for the NBS, KSBS, MTU, and w.MTU, when $R_k = 96$ kbps and $W_t = 20$ MHz, for all considered node distributions. In this case, NBS and KSBS assume $dp = (28, 28)^\top$ dB. The same results for the aforementioned criteria are also depicted in Table V, but for the case of $R_k = 96$ kbps and $W_t = 15$ MHz. In this case, NBS and KSBS assume $dp = (26, 26)^\top$ dB. The combination of the source–channel coding rate, and the power level of the high-motion class are represented as $(R_{s,1}, R_{c,1})$, and S_1, respectively, while $(R_{s,2}, R_{c,2})$ and S_2 are the corresponding parameters for the low-motion class.

First of all, all four criteria give a higher PSNR to the low-motion class of nodes compared to the high-motion class, with an exception observed for the MTU criterion, in cases where more nodes belong to the low-motion class. In such cases, the high-motion class achieves higher PSNR values than the low-motion class. The KSBS is a promising criterion, since it assigns close enough values to the PSNR of the two motion classes. Compared to the other schemes, the KSBS favors the high-motion class clearly more than the w.MTU and in many cases more than the NBS and MTU. This fact plays an important role, considering the significance of the scenes that include high levels of motion.

The MTU criterion guarantees the highest levels of total utility, cumulatively for both motion classes, compared to all other schemes. However, in cases where the cardinality of the low-motion class is smaller than this of the high-motion class, a large discrepancy between $PSNR_1$ and $PSNR_2$ is observed. Interpreting the results for the w.MTU, it favors eminently the low-motion class of nodes, offering clearly higher PSNR values compared to the NBS and KSBS, and even in some cases compared to the MTU. Interesting are the cases where the two motion classes include the same number of nodes. In such cases, both MTU and w.MTU offer exactly the same solution, i.e., the same PSNR values to both motion classes.

Regarding the power levels, for the NBS and KSBS we observe that the high-motion class of nodes requires higher power levels compared to the low-motion class, unlike w.MTU

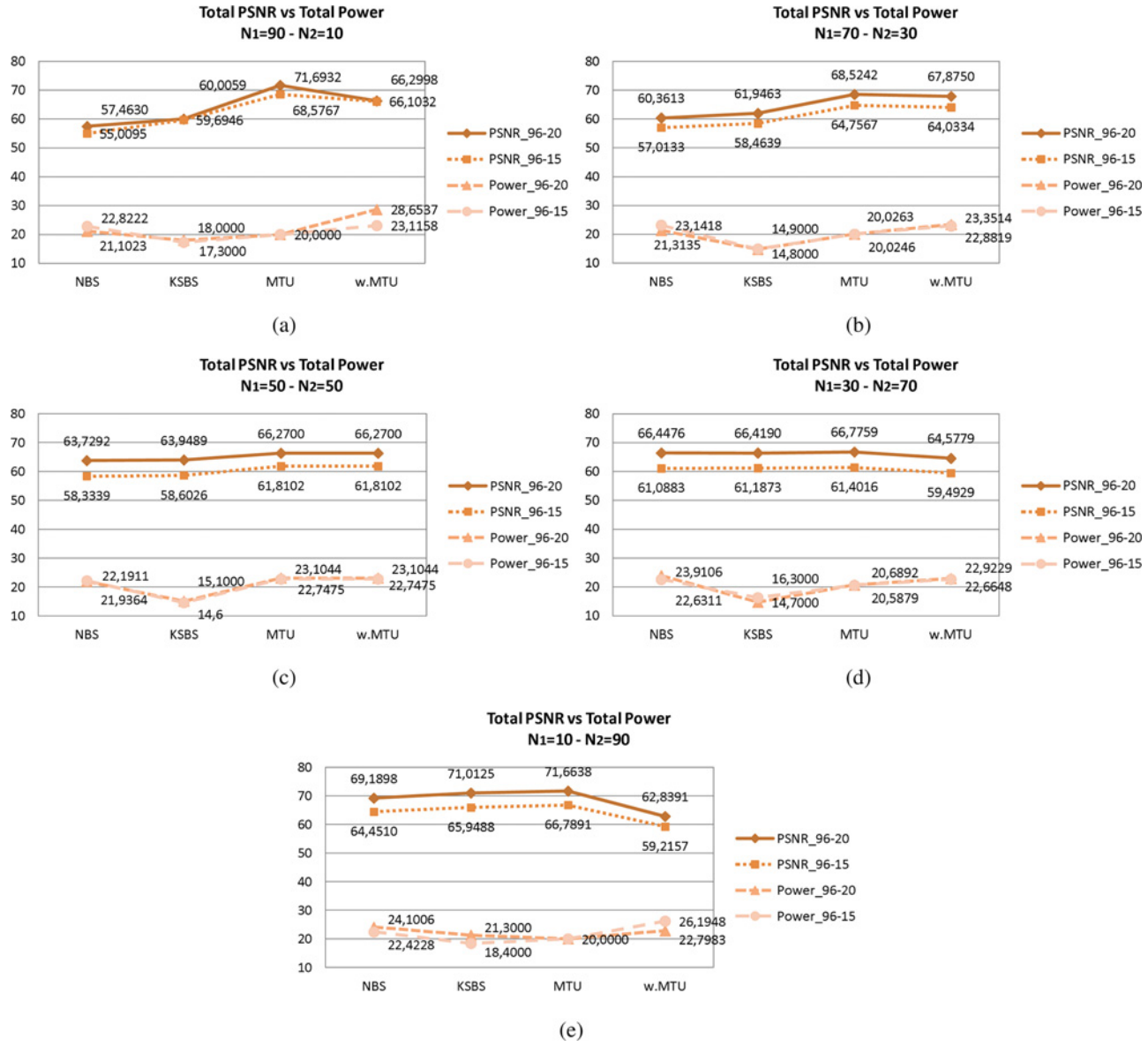

Fig. 3. Total PSNR gain versus total power consumption.

where the low-motion class maintains the highest power levels. For the MTU, we infer that the class that has the highest power level, achieves the highest PSNR. Also, for the source and channel coding rate combinations, since the total bit rate is assumed to be constant, a higher source coding rate means that fewer bits are available for channel coding, resulting in less error protection. Therefore, a higher power level is required in order to increase channel reliability, increasing at the same time the interference to the transmissions of the other nodes.

The PF values for the NBS, KSBS, and w.MTU are included in Table VI. Since the MTU was used as the reference criterion in (12), the PF values for this criterion are not defined. Moreover, as it was previously implied, in cases where the nodes are equally assigned to both motion classes, the w.MTU solutions coincide with the solutions of the MTU. Hence, in such cases the PF values are not defined either for the w.MTU.

The obtained PF results can be explained as follows. For every unit of utility lost by a class of nodes using the MTU, there are PF units of utility gained cumulatively for both motion classes, using also the MTU. The tendency of PF values for each scheme is similar for both considered combinations of bit rate and bandwidth, from node distribution to node distribution. Specifically, as the cardinality of the high-motion class decreases against the cardinality of the low-motion class, a PF decrease is observed, except for the case of "$10-90$" where the PF value is increased. Additionally, no specific scheme offers the highest or the lowest PF values in all node distributions. This always depends on the achieved PSNR values in each case. However, the conclusion derived using this metric is that the lower the PF value for a scheme, the smaller the discrepancy between the total achieved PSNR by the considered scheme and the MTU. Therefore, when the number of nodes that belong to the high-motion class increases, the utility gained cumulatively for both motion classes decreases.

Additional pieces of information are also provided by the graphical illustration of the results. Fig. 3 depicts the relation

TABLE III

PSNR RESULTS FOR THREE DIFFERENT dp ASSIGNMENTS PER BIT RATE AND BANDWIDTH COMBINATION

	R_k = 96 kbps, W_t = 20 MHz						R_k = 96 kbps, W_t = 15 MHz					
	$dp = (28, 28)^\top dB$		$dp = (26, 26)^\top dB$		$dp = (24, 24)^\top dB$		$dp = (26, 26)^\top dB$		$dp = (25, 25)^\top dB$		$dp = (24, 24)^\top dB$	
$N_1 - N_2$	$PSNR_1$	$PSNR_2$	$PSNR_1$	$PSNR_2$	$PSNR_1$	$PSNR_2$	$PSNR_1$	$PSNR_2$	$PSNR_1$	$PSNR_2$	$PSNR_1$	$PSNR_2$
90 − 10	28.2248	31.7811	27.6533	38.7737	27.4387	40.4599	26.3072	33.3874	26.0796	37.7415	25.9756	39.1441
70 − 30	29.0590	32.8873	28.3531	35.5374	28.0505	36.7516	26.7322	31.7317	26.3766	33.6255	26.1257	34.6615
50 − 50	30.3679	33.5810	29.5671	34.3620	29.2021	35.1549	27.6806	30.9220	27.2761	31.6966	27.0460	32.4253
30 − 70	32.0458	34.3732	31.5431	34.8620	31.2067	35.2058	29.5953	31.5920	29.2774	31.8243	29.0081	32.0654
10 − 90	34.9841	36.0284	34.7502	36.1288	34.5811	36.1992	32.9591	32.9897	32.8731	33.0132	32.7973	33.0311

TABLE IV

RESULTS FOR R_k = 96 KBPS, W_t = 20 MHZ. FOR THE NBS AND KSBS $dp = (28, 28)^\top dB$

	NBS						KSBS					
$N_1 - N_2$	$(R_{s,1}, R_{c,1})$	S_1	$(R_{s,2}, R_{c,2})$	S_2	$PSNR_1$	$PSNR_2$	$(R_{s,1}, R_{c,1})$	S_1	$(R_{s,2}, R_{c,2})$	S_2	$PSNR_1$	$PSNR_2$
90 − 10	(48, 1/2)	15.0000	(32, 1/3)	6.1023	28.3548	29.1082	(48, 1/2)	11.7000	(32, 1/3)	6.3000	28.2248	31.7811
70 − 30	(64, 2/3)	15.0000	(32, 1/3)	6.3135	29.5326	30.8287	(48, 1/2)	9.5000	(32, 1/3)	5.3000	29.0590	32.8873
50 − 50	(64, 2/3)	15.0000	(32, 1/3)	6.9364	30.9757	32.7535	(64, 2/3)	9.8000	(32, 1/3)	5.3000	30.3679	33.5810
30 − 70	(64, 2/3)	15.0000	(64, 2/3)	8.9106	31.2109	35.2367	(64, 2/3)	9.7000	(32, 1/3)	5.0000	32.0458	34.3732
10 − 90	(64, 2/3)	15.0000	(64, 2/3)	9.1006	32.2861	36.9037	(64, 2/3)	15.0000	(64, 2/3)	6.3000	34.9841	36.0284
	MTU						w.MTU					
$N_1 - N_2$	$(R_{s,1}, R_{c,1})$	S_1	$(R_{s,2}, R_{c,2})$	S_2	$PSNR_1$	$PSNR_2$	$(R_{s,1}, R_{c,1})$	S_1	$(R_{s,2}, R_{c,2})$	S_2	$PSNR_1$	$PSNR_2$
90 − 10	(32, 1/3)	5.0000	(64, 2/3)	15.0000	26.7244	44.9688	(48, 1/2)	13.6537	(64, 2/3)	15.0000	27.6931	38.6067
70 − 30	(32, 1/3)	5.0246	(64, 2/3)	15.0000	25.3578	43.1664	(32, 1/3)	8.3514	(64, 2/3)	15.0000	26.5871	41.2879
50 − 50	(32, 1/3)	8.1044	(64, 2/3)	15.0000	25.9290	40.3410	(32, 1/3)	8.1044	(64, 2/3)	15.0000	25.9290	40.3410
30 − 70	(64, 2/3)	15.0000	(32, 1/3)	5.6892	33.5507	33.2252	(32, 1/3)	7.9229	(64, 2/3)	15.0000	25.2663	39.3116
10 − 90	(64, 2/3)	15.0000	(64, 2/3)	5.0000	36.3876	35.2762	(32, 1/3)	7.7983	(64, 2/3)	15.0000	24.6122	38.2269

TABLE V

RESULTS FOR R_k = 96 KBPS, W_t = 15 MHZ. FOR THE NBS AND KSBS $dp = (26, 26)^\top dB$

	NBS						KSBS					
$N_1 - N_2$	$(R_{s,1}, R_{c,1})$	S_1	$(R_{s,2}, R_{c,2})$	S_2	$PSNR_1$	$PSNR_2$	$(R_{s,1}, R_{c,1})$	S_1	$(R_{s,2}, R_{c,2})$	S_2	$PSNR_1$	$PSNR_2$
90 − 10	(32, 1/3)	15.0000	(32, 1/3)	7.8222	26.4914	28.5181	(32, 1/3)	9.1000	(32, 1/3)	8.2000	26.3072	33.3874
70 − 30	(32, 1/3)	15.0000	(32, 1/3)	8.1418	26.9339	30.0794	(32, 1/3)	8.9000	(32, 1/3)	6.0000	26.7322	31.7317
50 − 50	(48, 1/2)	15.0000	(32, 1/3)	7.1911	27.9503	30.3836	(48, 1/2)	9.6000	(32, 1/3)	5.0000	27.6806	30.9220
30 − 70	(48, 1/2)	15.0000	(32, 1/3)	7.6311	29.0261	32.0622	(64, 2/3)	11.2000	(32, 1/3)	5.1000	29.5953	31.5920
10 − 90	(64, 2/3)	15.0000	(32, 1/3)	7.4228	31.0886	33.3624	(64, 2/3)	13.2000	(32, 1/3)	5.2000	32.9591	32.9897
	MTU						w.MTU					
$N_1 - N_2$	$(R_{s,1}, R_{c,1})$	S_1	$(R_{s,2}, R_{c,2})$	S_2	$PSNR_1$	$PSNR_2$	$(R_{s,1}, R_{c,1})$	S_1	$(R_{s,2}, R_{c,2})$	S_2	$PSNR_1$	$PSNR_2$
90 − 10	(32, 1/3)	5.0000	(64, 2/3)	15.0000	25.3543	43.2224	(32, 1/3)	8.1158	(64, 2/3)	15.0000	25.8689	40.2343
70 − 30	(32, 1/3)	5.0263	(64, 2/3)	15.0000	23.7017	41.0550	(32, 1/3)	7.8819	(64, 2/3)	15.0000	25.0542	38.9792
50 − 50	(32, 1/3)	7.7475	(64, 2/3)	15.0000	24.2297	37.5805	(32, 1/3)	7.7475	(64, 2/3)	15.0000	24.2297	37.5805
30 − 70	(64, 2/3)	15.0000	(32, 1/3)	5.5879	30.7752	30.6264	(32, 1/3)	7.6648	(64, 2/3)	15.0000	23.3987	36.0942
10 − 90	(64, 2/3)	15.0000	(32, 1/3)	5.0000	34.1215	32.6676	(32, 1/3)	11.1948	(32, 1/3)	15.0000	24.9082	34.3075

TABLE VI

PF VALUES PER BIT RATE AND BANDWIDTH COMBINATION

	R_k = 96 kbps, W_t = 20 MHz			R_k = 96 kbps, W_t = 15 MHz		
$N_1 - N_2$	NBS	KSBS	w.MTU	NBS	KSBS	w.MTU
90 − 10	8.7280	7.7895	5.5677	11.9314	9.3211	4.8066
70 − 30	1.9553	1.7772	0.5281	2.3957	2.0765	0.5348
50 − 50	0.5035	0.5229	–	0.9343	0.9295	–
30 − 70	0.1632	0.3109	0.3611	0.2182	0.2219	0.3491
10 − 90	1.5201	0.8659	2.9907	3.3651	2.6088	4.6182

between the total achieved utility and the total consumed power, for all examined criteria. Each subfigure refers to a specific node distribution and presents the results for both considered bit rate and bandwidth combinations. As we observe, the tendency of the total utility as well as that of the total power consumption is similar for both considered bit rate and bandwidth combinations. Specifically, the sum of the PSNR values is reduced in all criteria and node distributions, when the bandwidth is reduced (keeping the bit rate constant), since in such a case the value of (2) decreases. For the sum of the power levels, there is no noticeable difference between the two considerations for the bandwidth.

From Fig. 3, we also observe that no scheme simultaneously holds the desired features of achieving the highest levels of utility and consuming the lowest levels of power, cumulatively for both motion classes. Clearly, such a scheme would be a preferable scheme. Although the MTU assures the highest levels of utility, it is an unfair scheme if we consider the amounts of consumed power as well as the high discrepancy that is often observed in the PSNR values of the two motion classes. Alternatively, if we are interested in achieving similar PSNR values for both motion classes, we could say that in some cases the NBS is the most suitable criterion, while in some other cases the MTU meets this requirement. Despite all these, neither the NBS nor the MTU can be considered as equally fair criteria to both motion classes, if we also consider the power levels required by each motion class. In cases of similar PSNR values, the high-motion class is undoubtedly more demanding in resources.

The KSBS that is proposed in this paper is a compromise to all our requirements. The main strength of this method is that it guarantees the lowest power level values, cumulatively for both motion classes, far exceeding the other competing methods. Additionally, it assigns close PSNR values to both motion classes compared to the values assigned by the MTU and w.MTU and even by the NBS, in cases where the cardinality of the low-motion class is greater than that of the high-motion one. Also, the KSBS clearly outperforms the NBS in terms of the total utility gained by both motion classes, and in cases where more nodes belong to the low-motion class, it also outperforms the w.MTU.

VIII. Conclusion

In this paper, we addressed the problem of optimal resource allocation among the nodes of a wireless DS-CDMA VSN, considering a number of assumptions and constraints. Specifically, we optimally determined the discrete source and channel coding rates, and the continuous power levels of the nodes, aiming at the amelioration of the video quality that reaches the end-user. The CCU is able to request changes in nodes' transmission parameters according to their needs for compression and protection, using a flexible cross-layer design.

The Kalai–Smorodinsky bargaining solution is invoked to deal with the aforementioned problem. This solution, based on its fairness axioms, provides a fair and efficient rule that assigns the transmission parameters to each node. In our problem, this solution was derived geometrically, based on the graphical representation of each considered feasible set, implying low running complexity. The performance of the KSBS was assessed in comparison with three competing criteria: the Nash bargaining solution and two other methods that attempt to maximize an unweighted and a weighted version of the total system utility, respectively.

For the quality evaluation of the methods, we used a metric that captures both fairness and performance issues. This metric expressed the total utility gain achieved by all nodes using the MTU, that is attributed to every unit of utility lost by an isolated node, using also the MTU. Additionally, we studied the total utility achieved cumulatively from all nodes in combination with the total power consumption, for each scheme. No scheme gathered all desired features of being equally fair to all nodes, assuring the highest total utility, and requiring the lowest levels of power, at the same time. Nevertheless, comparisons led us to the conclusion that the KSBS is the criterion that is closer to our demands. The main strength of this method is that it assures quite low levels of power consumption, while assigning close enough PSNR values to all nodes and having low running complexity at the same time.

References

[1] L. P. Kondi and E. S. Bentley, "Game-theory-based cross-layer optimization for wireless DS-CDMA visual sensor networks," in *Proc. 17th IEEE ICIP*, Sep. 2010, pp. 4485–4488.

[2] K. Pandremmenou, L. P. Kondi, and K. E. Parsopoulos, "Optimal power allocation and joint source–channel coding for wireless DS-CDMA visual sensor networks using the Nash bargaining solution," in *Proc. 36th ICASSP*, May 2011, pp. 2340–2343.

[3] K. Pandremmenou, L. P. Kondi, and K. E. Parsopoulos, "Optimal power allocation and joint source–channel coding for wireless DS-CDMA visual sensor networks," in *Proc. SPIE Electronic Imaging Symp. (Visual Inform. Process. Commun. II)*, vol. 7882. May 2011, pp. 2340–2343.

[4] E. S. Bentley, L. P. Kondi, J. D. Matyjas, M. J. Medley, and B. W. Suter, "Spread spectrum visual sensor network resource management using an end-to-end cross-layer design," *IEEE Trans. Multimedia*, vol. 13, no. 1, pp. 125–131, Feb. 2011.

[5] J. Suris, L. Dasilva, Z. Han, A. Mackenzie, and R. Komali, "Asymptotic optimality for distributed spectrum sharing using bargaining solutions," *IEEE Trans. Wireless Commun.*, vol. 8, no. 10, pp. 5225–5237, Oct. 2009.

[6] B. Yang, Y. Shen, G. Feng, and X. Guan, "Fair resource allocation using bargaining over OFDMA relay networks," in *Proc. CDC*, 2009, pp. 585–590.

[7] H. Park and M. van der Schaar, "Bargaining strategies for networked multimedia resource management," *IEEE Trans. Signal Process.*, vol. 55, no. 7, pp. 3496–3511, Jul. 2007.

[8] H. Park and M. van der Schaar, "Fairness strategies for wireless resource allocation among autonomous multimedia users," *IEEE Trans. Circuits Syst. Video Technol.*, vol. 20, no. 2, pp. 297–309, Feb. 2010.

[9] M. Khan, C. Truong, T. Geithner, F. Sivrikaya, and S. Albayrak, "Network level cooperation for resource allocation in future wireless networks," in *Proc. 1st IFIP WD*, Nov. 2008, pp. 1–5.

[10] J. Chen and A. Swindlehurst, "Downlink resource allocation for multiuser MIMO–OFDMA systems: The Kalai-Smorodinsky bargaining approach," in *Proc. 3rd IEEE Int. Workshop CAMSAP*, Dec. 2009, pp. 380–383.

[11] N. Mastronarde and M. van der Schaar, "A bargaining theoretic approach to quality-fair system resource allocation for multiple decoding tasks," *IEEE Trans. Circuits Syst. Video Technol.*, vol. 18, no. 4, pp. 453–466, Apr. 2008.

[12] A. Fattahi and F. Paganini, "New economic perspectives for resource allocation in wireless networks," in *Proc. 2005 American Control Conf.*, vol. 6. Jun. 2005, pp. 3960–3965

[13] M. Khan, A. Toker, C. Troung, F. Sivrikaya, and S. Albayrak, "Cooperative game theoretic approach to integrated bandwidth sharing and allocation," in *Proc. Int. Conf. GameNets*, May 2009, pp. 1–9.
[14] H. Park and M. van der Schaar, "Congestion game modeling for brokerage based multimedia resource management," in *Proc. Packet Video*, Nov. 2007, pp. 18–25.
[15] A. Ibing and H. Boche, "Fairness vs. efficiency: Comparison of game theoretic criteria for OFDMA scheduling," in *Proc. Conf. Record Forty—1st Asilomar Conf. Signals, Syst. Comput.*, Nov. 2007, pp. 275–279.
[16] G. Tan, "Improving aggregate user utilities and providing fairness in multi-rate wireless LANs," Ph.D. dissertation, Massachusetts Inst. Technol. (MIT), Cambridge, MA, USA, 2006.
[17] K. Pandremmenou, L. P. Kondi, and K. E. Parsopoulos, "Fairness issues in resource allocation schemes for wireless visual sensor networks," in *Proc. SPIE Electron. Imaging Symp. (Visual Inform. Process. Commun. III)*, vol. 8666. Feb. 2013.
[18] K. Pandremmenou, L. P. Kondi, and K. E. Parsopoulos, "Kalai–Smorodinsky bargaining solution for optimal resource allocation over wireless DS-CDMA visual sensor networks," in *Proc. SPIE Electron. Imaging Symp. (Visual Inform. Process. Commun. III)*, vol. 8305. 2012.
[19] U. Endriss, N. Maudet, F. Sadri, and F. Toni, "On optimal outcomes of negotiations over resources," in *Proc. 2nd Int. Joint Conf. Autonomous Agents Multiagent Syst.* 2003, pp. 177–184.
[20] W. S. Lin, H. V. Zhao, and K. J. R. Liu, "Fairness dynamics in multimedia colluders' social networks," in *Proc. 15th IEEE ICIP*, vol. 1–5. 2008, pp. 3132–3135.
[21] H. Ganapathy, S. Banerjee, N. Dimitrov, and C. Caramanis, "Optimal feedback allocation algorithms for multi-user uplink," in *Proc. 47th Annu. Allerton Conf. Commun., Control, Computing*, 2009, pp. 947–954.
[22] J. Wang, T. Korhonen, and Y. Zhao, "Weighted network utility maximization aided by combined queueing priority in OFDMA systems," in *Proc. IEEE ICC*, May 2008, pp. 3323–3327.
[23] C. Weeraddana, W. Li, M. Codreanu, and M. Latva-aho, "Weighted sum-rate maximization for downlink OFDMA systems," in *Proc. 42nd Asilomar Conf. Signals, Syst. Comput., 2008*, Oct. 2008, pp. 990–994.
[24] J. Kennedy and R. C. Eberhart, "Particle swarm optimization," in *Proc. IEEE Int. Conf. Neural Netw.*, vol. IV. Nov./Dec. 1995, pp. 1942–1948.
[25] R. C. Eberhart and J. Kennedy, "A new optimizer using particle swarm theory," in *Proc. 6th Symp. Micro Mach. Human Sci.*, 1995, pp. 39–43.
[26] L. P. Kondi, F. Ishtiaq, and A. K. Katsaggelos, "Joint source-channel coding for motion–compensated DCT-based SNR scalable video," *IEEE Trans. Image Process.*, vol. 11, no. 9, pp. 1043–1052, Sep. 2002.
[27] T. Rappaport, *Wireless Communications: Principles and Practice*, 2nd ed. Upper Saddle River, NJ, USA: Prentice-Hall PTR, 2001.
[28] Y. S. Chan and J. Modestino, "A joint source coding-power control approach for video transmission over CDMA networks," *IEEE J. Selected Areas Commun.*, vol. 21, no. 10, pp. 1516–1525, Dec. 2003.
[29] H. Wang, L. P. Kondi, A. Luthra, and S. Ci, *4G Wireless Video Communications*. New York, USA: Wiley Publishing, 2009.
[30] J. Hagenauer, "Rate-compatible punctured convolutional codes (RCPC codes) and their applications," *IEEE Trans. Commun.*, vol. 36, no. 4, pp. 389–400, Apr. 1988.
[31] M. Bystrom and T. Stockhammer, "Modeling of operational distortion-rate characteristics for joint source–channel coding of video," in *Proc. ICIP*, vol. 1. 2000, pp. 359–362.
[32] H. J. M. Peters, *Axiomatic Bargaining Game Theory*. Norwell, MA, USA: Kluwer Academic Publishers, 1992.
[33] K. Binmore, *Playing for Real: A Text on Game Theory*. Oxford, U.K.: Oxford University Press, 2007.
[34] J. P. Conley and S. Wilkie, "The bargaining problem without convexity: Extending the egalitarian and Kalai–Smorodinsky solutions," *Economic Lett.*, vol. 36, no. 4, pp. 365–369, Aug. 1991.
[35] E. Kalai and M. Smorodinsky, "Other solutions to Nash's bargaining problem," *Econometrica*, vol. 43, no. 3, pp. 513–518, 1975.

Katerina Pandremmenou (S'11) received the B.Sc. degree in computer science in 2008 from the Computer Science Department, University of Crete, Crete, Greece. In 2011, she received the M.Sc degree in technologies-applications from the Computer Science Department, University of Ioannina, Ioannina, Greece, where she is currently pursuing the Ph.D. degree.

Her current research interests include video compression and transmission over wireless networks, and video quality metrics.

Lisimachos P. Kondi (SM'11) received the Diploma in electrical engineering from the Aristotle University of Thessaloniki, Thessaloniki, Greece, in 1994, and the M.S. and Ph.D. degrees in electrical and computer engineering from Northwestern University, Evanston, IL, USA, in 1996 and 1999, respectively.

During the 1999–2000 academic year, he was a Post-Doctoral Research Associate at Northwestern University. He is currently an Assistant Professor with the Department of Computer Science, University of Ioannina, Greece. He was previously with the faculty of the University at Buffalo, The State University of New York, Buffalo, NY, USA, and has also held appointments at the Naval Research Laboratory, Washington, DC, USA, and the Air Force Research Laboratory, Rome, NY, USA. His current research interests include the general areas of signal and image processing and communications, including image and video compression and transmission over wireless channels and the Internet, superresolution of video sequences, and shape coding.

Dr. Kondi is an Associate Editor of the *EURASIP Journal on Advances in Signal Processing* and has served as Associate Editor of the IEEE SIGNAL PROCESSING LETTERS.

Konstantinos E. Parsopoulos (M'05) serves as Assistant Professor at the Department of Computer Science, University of Ioannina, Ioannina, Greece.

He has authored one book and more than 80 papers in scientific journals, conferences and edited volumes, while it has received more than 2000 citations. His current research interests include computational optimization and modeling with an emphasis on metaheuristics and high-performance algorithms.